JPE 17-2-14

https://doi.org/10.6113/JPE.2017.17.2.453
ISSN(Print): 1598-2092 / ISSN(Online): 2093-4718

Reduced Order Identification and Stability Analysis of DC-DC Converters

Husan Ali†, Xiancheng Zheng*, Xiaohua Wu*, Haider Zaman*, and Shahbaz Khan*

†,*School of Automation, Northwestern Polytechnical University, Xi'an, China

Abstract

This paper discusses the measurement of frequency response functions for various dc-dc converters. The frequency domain identification procedure is applied to the measured frequency responses. The identified transfer functions are primarily used in developing behavioral models for dc-dc converters. Distributed power systems are based upon such converters in cascade, parallel and several other configurations. The system level analysis of a complete system becomes complex when the identified transfer functions are of high order. Therefore, a certain technique needs to be applied for order reduction of the identified transfer functions. During the process of order reduction, it has to be ensured that the system retains the dynamics of the full order system. The technique used here is based on the Hankel singular values of a system. A systematic procedure is given to retain the maximum energy states for the reduced order model. A dynamic analysis is performed for behavioral models based on full and reduced order frequency responses. The close agreement of results validates the effectiveness of the model order reduction. Stability is the key design objective for any system designer. Therefore, the measured frequency responses at the interface of the source and load are also used to predict stability of the system.

Key words: DC-DC converter, Nyquist criterion, Order reduction, Stability, System identification

I. INTRODUCTION

Switched-Mode Power Supplies (SMPS) are being used in several electronic applications [1], [2]. The pre-requisite for all of the design approaches regarding the analysis of SMPS is to have complete knowledge about the internal structure and parameters of the converter [3], [4]. Designers often have very limited information available for modeling these converters. This issue is commonly faced in Distributed Power Systems (DPSs) where different modules such as converters, filters and loads are designed by different vendors.

This leads us to the behavioral or black-box modeling approach [5]. Behavioral modeling is a popular approach for the system level design and analysis of distributed power systems. In black-box modeling a frequency response analyzer, commonly known as network analyzer is used to measure the set of frequency responses called g-parameters which are used for the construction of black-box models. The advantage of this modeling approach is that various models can be easily interconnected in different configurations i.e. in cascade and parallel form. Such power distribution systems are widely found in telecommunication applications, data communication systems, more electric aircraft, electric vehicles, etc. [6]-[8].

The first step in the development of a black-box model for any system is to carry out frequency response measurements. Then system identification procedure is applied to the measured frequency responses to get the transfer functions. The g-parameter transfer functions obtained via the system identification procedure from the measured frequency responses are rather high in order. In case of distributed power systems where there is a number of subsystems, the high order of identified transfer functions makes the system level analysis much more challenging. Hence, there is need to obtain low order models. The order reduction of a transfer function can achieve several goals, including simplification of the model and speeding up of the simulation process. During the order reduction process, it needs to be ensured that the states of systems with maximum energy are preserved. The obtained reduced order transfer functions can be used for the analysis of distributed power systems without significant loss of information.

Manuscript received Jun. 6, 2016; accepted Jan. 23, 2017
Recommended for publication by Associate Editor Sung-Jin Choi.
†Corresponding Author: engr.husan@gmail.com
Tel: +86-1874-0476-759, Northwestern Polytechnical University
*School of Automation, Northwestern Polytechnical University, China

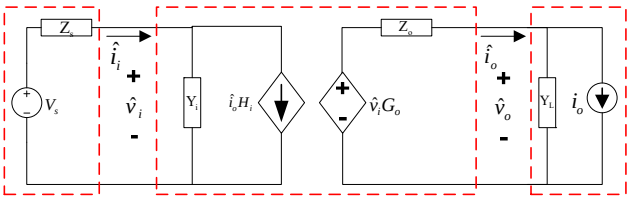

Fig. 1. Two port network model for dc-dc converter.

The frequency response measurements and transfer function derivation via system identification, both full order and reduced order, was done for a prototype dc-dc buck converter in [9]. This work extends this concept further to a prototype dc-dc boost converter and a commercial isolated dc-dc converter. The model order reduction methods e.g. the pole-zero cancellation technique and singular perturbations are more suitable only for systems where enough information is available about the internal dynamics of the system, which is not always the case. In this study, a Hankel singular values based method is used. Furthermore, a systematic procedure is developed and used to determine the maximum energy states to be retained for a low order model. After obtaining the full and reduced order transfer functions, a time domain validation is done by building behavioral models based upon the full and reduced order frequency responses. The step load current test is applied to the behavioral model to analyze and compare the responses of the full and reduced order models. In addition, a comparison of the simulation speeds for full and reduced order transfer function based behavioral models shows that the reduced order transfer functions based models are computationally more efficient and require a lot less simulation time.

The integration of various modules from different vendors into a distributed power architecture results in complex dynamic behavior of the system. It also sometimes gives rise to concerns regarding the stability of the overall system. In this study, the stability of the system is analyzed using small signal impedance based stability criterion. The source output impedance and load input admittance are measured at the interface of source and load. They are then used to predict the stability of the system.

II. Two Port Model of DC-DC Converters

Two port models have been extensively applied for the analysis of dc-dc converters [10]-[12]. In the use of linear two port representation based on g-parameters, the parameters represent the real internal dynamics excluding the source and load effects. The input and output port parameters constitute a set known as g-parameters.

The input port is represented by a Norton equivalent circuit while the output port is represented by a Thevenin equivalent circuit as shown in Fig. 1 [5].

A two port network model is used to build a small signal linear model of a dc-dc converter around a particular operating point. The four transfer functions required for the behavioral model are the input admittance, back current gain, audiosusceptibility and output impedance denoted by Y_i, H_i, G_o and Z_o, respectively. Mathematically the g-parameter set can be written as shown in equation (1).

$$Y_i = \left.\frac{\hat{i}_i}{\hat{v}_i}\right|_{i_o=0} \quad H_i = \left.\frac{\hat{i}_i}{\hat{i}_o}\right|_{v_i=0}$$
$$G_o = \left.\frac{\hat{v}_o}{\hat{v}_i}\right|_{i_o=0} \quad Z_o = \left.\frac{\hat{v}_o}{\hat{i}_o}\right|_{v_i=0} \tag{1}$$

The small signal input variables of the two port model are the input voltage and output current $(\hat{v}_i, \hat{i}_o)$while the small signal output variables are the output voltage and input current $(\hat{v}_o, \hat{i}_i)$. In terms of these variables, the two port network model of Fig. 1 can be represented as:

$$\begin{bmatrix}\hat{i}_i \\ \hat{v}_o\end{bmatrix} = \begin{bmatrix}Y_i & H_i \\ G_o & -Z_o\end{bmatrix}\begin{bmatrix}\hat{v}_i \\ \hat{i}_o\end{bmatrix} \tag{2}$$

The negative sign in equation (2) is due to the direction of output current as shown in Fig. 1.

III. Frequency Response Measurements

To measure the frequency response of a power supply, certain signals need to be perturbed. The source of the network analyzer generates a sinusoidal perturbation signal to be injected into the circuit through an isolation transformer. The injected signal is used to perturb the input voltage or output current. The perturbation signal is amplified before injection into the circuit. The amplitude of the injection signal should not be too small, so that it is dominated by noise, or too large, which would affect the normal operation of the circuit.

An Agilent's network analyzer E5061B, which has a frequency range of 5Hz-3GHz, is used in this study to measure the frequency response of the system [13]. The measurement results plot the gain and phase as a function of the frequency. It is important to mention that the measurements made by network analyzer are valid up to half of the switching frequency. Measurements after half of a switching frequency are not reliable since the aliasing phenomenon becomes an issue [14].

The measurement setup in Fig. 2, is used for the measurement of the input admittance and audiosusceptibility. For introducing perturbation into the input voltage, an injection signal is connected in series with the source. For both of these measurements, channel R measures the input voltage. For input admittance, channel T measures the input current so that the ratio (C/B) gives the input admittance $(\hat{\imath}_i/\hat{v}_i)$. For audiosusceptibility, channel T measures the output voltage so that the ratio (A/B) gives audiosusceptibility $(\hat{v}_o/\hat{v}_i)$.

The measurement setup in Fig. 3, is used for the measurement of the output impedance and back current gain. For introducing a perturbation into the output current, the injection signal is connected in parallel across the load. For

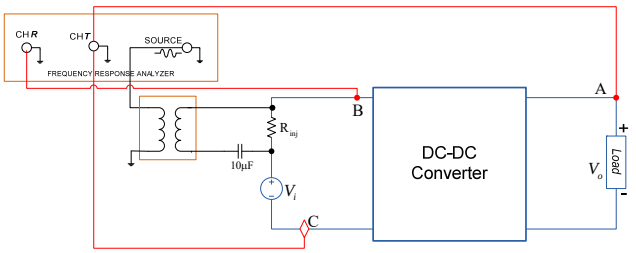

Fig. 2. Measurement setup for input admittance and audiosusceptibility.

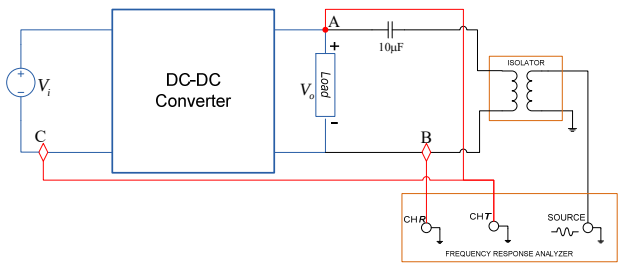

Fig. 3. Measurement setup for output impedance and back current gain.

both of these measurements, channel R measures the output current. For the output impedance, channel T measures the output voltage so that the ratio (A/B) gives the output impedance ($\hat{v}_o/\hat{i}_o$). For the back current gain, channel T measures the input current so that the ratio (C/B) gives the back current gain ($\hat{i}_i/\hat{i}_o$).

IV. Identification of Measured Frequency Response Functions

The identification process deals with the identification of transfer functions from the measured frequency response data [15]. The MATLAB software package is used to get the identified transfer functions. The measured frequency responses are imported to MATLAB and the command *csvread* is used to read the data from the imported files. The magnitude and phase data is changed into complex form, while frequency to rad/s, for the creation of a data object in the next step. The data object is created using the command *frd* from the magnitude and phase data in complex form, the frequency values in rad/s and the sampling time which is zero for a continuous system.

data_object = frd (response, frequency, Ts)

The most important step is to choose a model from the available set of models to fit the data. Some of the commonly used models are *FRD, ARX, OE* and *PEM*. In this study, the state space model based structure *FRD* is used. The MATLAB command *fitfrd* is used to achieve this. The data object created in the previous step and the required order of the transfer function are provided as arguments.

model_frd = fitfrd (data_object, order)

Normally a few iterations are required to best fit the identified result into the measured data. Fig. 4 gives a summary of the steps involved in the identification process.

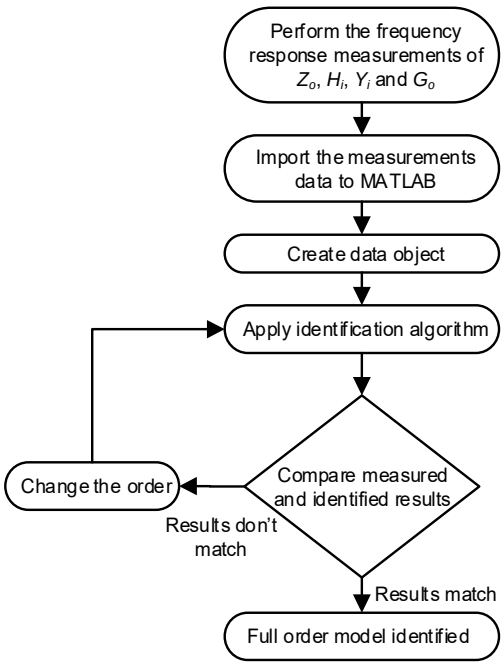

Fig. 4. Algorithm to obtain identified transfer functions.

V. Measured and Identified Frequency Response Results

The frequency response functions obtained through the system identification procedure discussed above are compared with the measurement results and presented for three dc-dc converters.

The output impedance frequency response measurement contains information regarding the response of the converter to dynamic load changes at different frequencies. The output impedance shows how a converter regulates and responds to various load changes. The output impedance gives ideas about any changes in the load, while the input admittance does so concerning any interaction from the source. This determines the sensitivity of a power system to input filter or input power components. The input admittance measurement gives the designer idea about the integration of a power supply into another system. An audiosusceptibility frequency response measurement determines the transmission of noise from the input of the system to the output. It tells about the ability of the converter to reject noise appearing at the input. Compared to the output impedance and back current gain it is more difficult to measure the audiosusceptibility and input admittance because the small signal injection is in series with the DC source [16]. Fig. 5 shows a comparison of the measured and identified frequency response plots of the four g-parameters for a prototype buck converter, whose parameters are given in Table I.

TABLE I
BUCK CONVERTER PARAMETERS

Input Voltage	Inductor	Capacitor	Output Voltage	Output Power	Switching Frequency
V_{in}	L	C	V_{out}	P_o	f_s
$20V$	$100\mu H$	$320\mu F$	$10V$	$20W$	$100kHz$

TABLE II
BOOST CONVERTER PARAMETERS

Input Voltage	Inductor	Capacitor	Output Voltage	Output Power	Switching Frequency
V_{in}	L	C	V_{out}	P_o	f_s
$20V$	$350\mu H$	$330\mu F$	$30V$	$50W$	$100kHz$

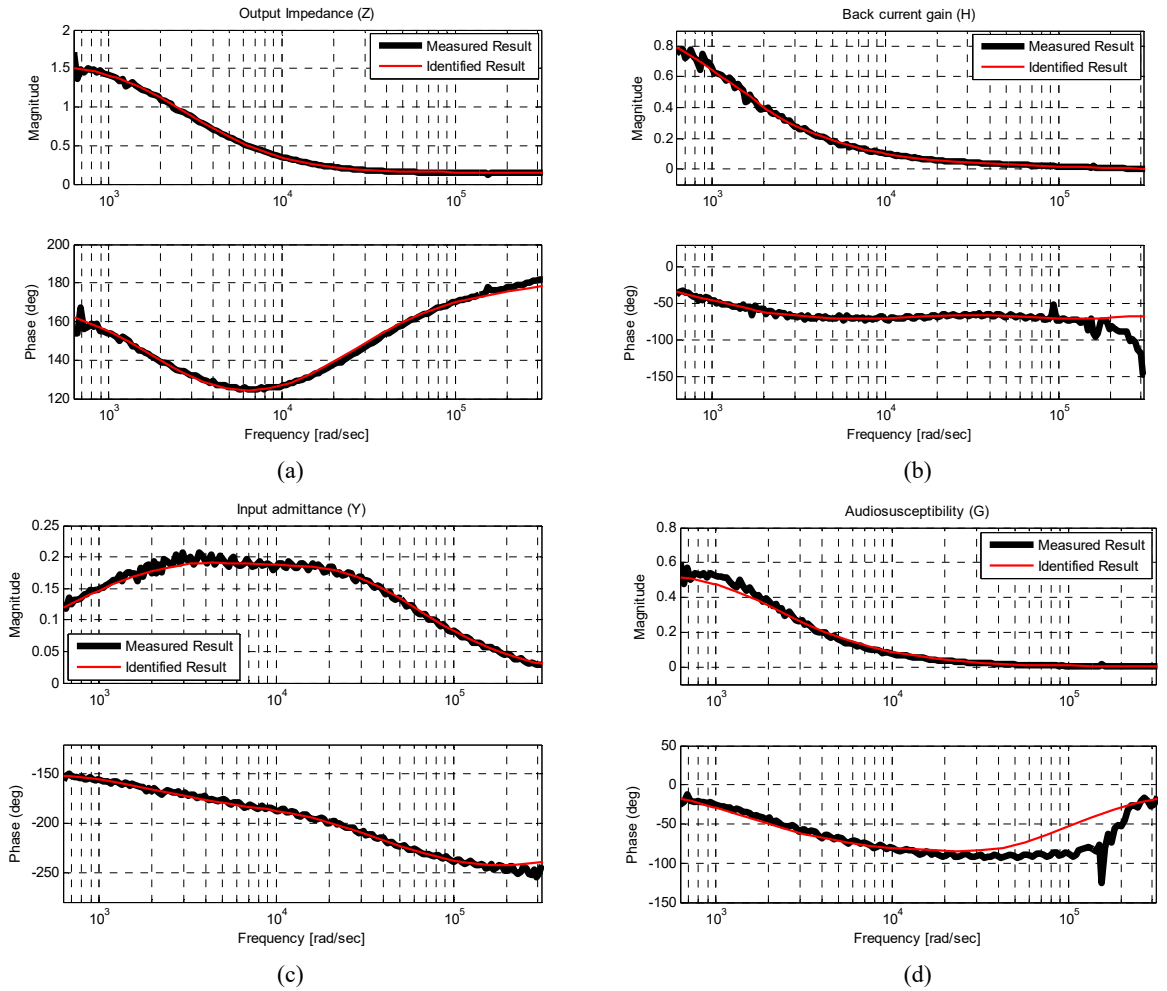

Fig. 5. Frequency response comparison of (a) Output impedance (b) Back current gain (c) Input admittance (d) Audiosusceptibility.

Fig. 6 shows a comparison of the measured and identified frequency response plots of the four g-parameters for a prototype boost converter, whose parameters are given in Table II.

To further validate the procedure for the measurement and identification of frequency response functions, a commercially available converter *V24C5C100BL* is used [17]. The 100W, 24/5V converter's high frequency ZCS/ZVS switching provides a high power density with a low noise and a high efficiency. Fig. 7 shows a comparison of the measured and identified frequency response plots of the four g-parameters for a commercial dc-dc converter.

The results clearly show that the identified models closely match the measured frequency response functions in the given frequency range of interest.

VI. FREQUENCY RESPONSE FUNCTIONS FOR REDUCED ORDER MODELS

System order reduction is a mathematical process that aims to replace high order transfer functions with transfer functions of considerably lower dimensions, while ensuring that it has the same response characteristics. Two methods which can be employed for system order reduction are the pole-zero cancellation technique and the Hankel singular values based method.

A. Pole-Zero Cancellation Technique

The pole-zero cancellation technique is a relatively simple technique, which can be easily employed if a pole is located at exactly the same point as a zero [18]. It may seem all right to cancel a pole and a zero if they are close to each other.

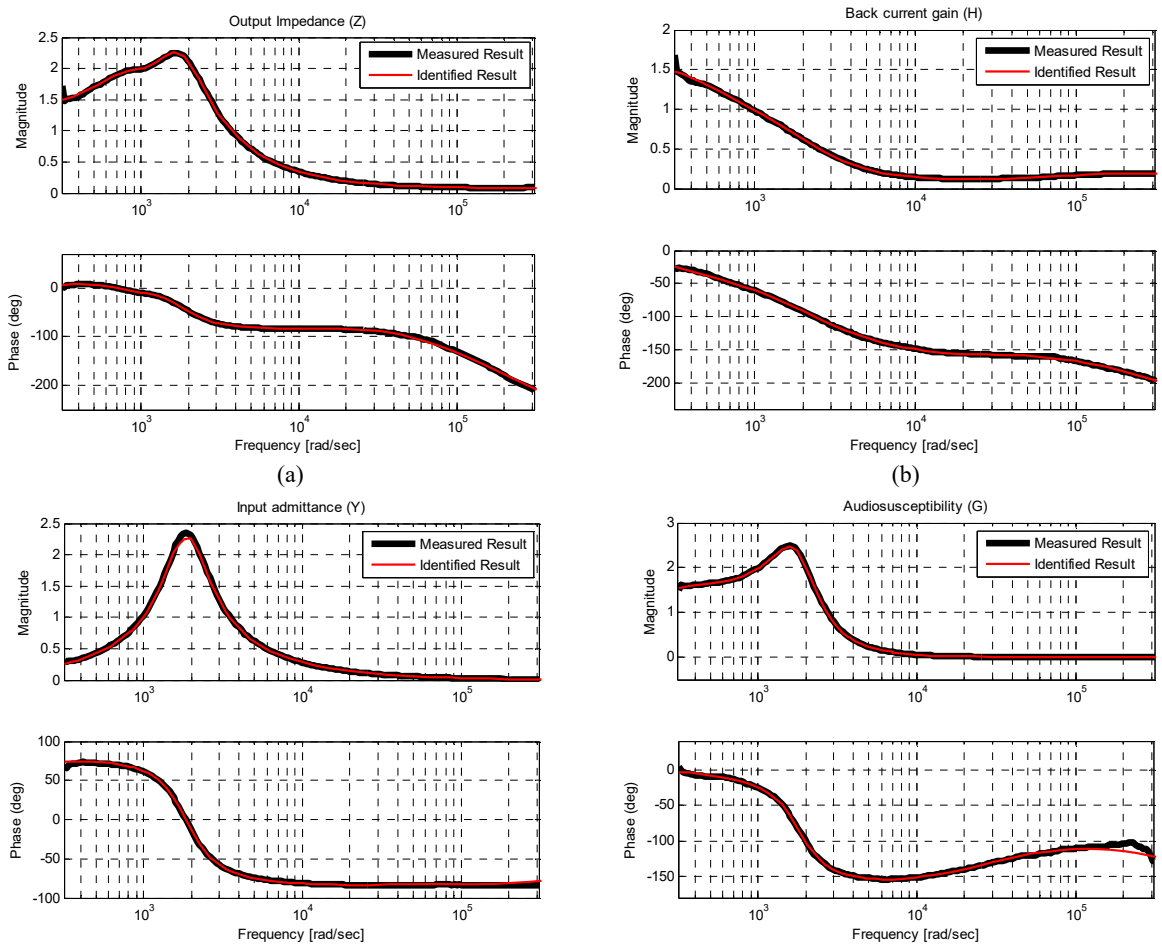

Fig. 6. Frequency response comparison of (a) Output impedance (b) Back current gain (c) Input admittance (d) Audiosusceptibility.

However, in order to achieve this, it is necessary to have information about the dynamics of the system. The poles and zeros that are associated with the dominant dynamics of the system cannot be cancelled even if they are apparently located close to each other. This technique is more suitable for models where the relationship between different parameters and certain states is well known.

The output impedance of the buck converter shown in Fig. 5 (a) is identified with the 3rd order transfer function given in equation (3).

$$Z_o(s) = \frac{-0.183\ (s+1.916e006)\ (s+2.103e004)\ (s+98.29)}{(s+2.332e006)\ (s+2014)\ (s+72.68)} \qquad (3)$$

The MATLAB command *minreal* is used to cancel the pole-zero pairs in transfer functions. It can be applied equally to eliminate uncontrollable and unobservable states for state-space models.

model_reduced = minreal (mod_full)

Since there are no poles and zeros having the same value, it results in the same transfer function as above. However, it will be shown next that the order of Z_o can be reduced while preserving the dominant dynamics of the system.

B. Hankel Singular Values Based Method

For transfer functions obtained via identification, as is the case in this study, the pole-zero cancellation technique is not effective because the converter parameters and the identified models cannot be directly related. In order to overcome this drawback, a reduction technique based upon the Hankel singular values of the system is employed. Hankel singular values are parameters which determine the energy contained by each state of a system. During the process of transfer function order reduction it is important to keep the states with high energy so that the main features, e.g. dynamic response and stability, are preserved. The Hankel singular values based system order reduction technique presented here, can achieve a reduced order model that preserves the important system characteristics.

In control theory, eigenvalues define the system stability, whereas Hankel singular values define the energy of each state of a system. The general state space representation of a system is given as:

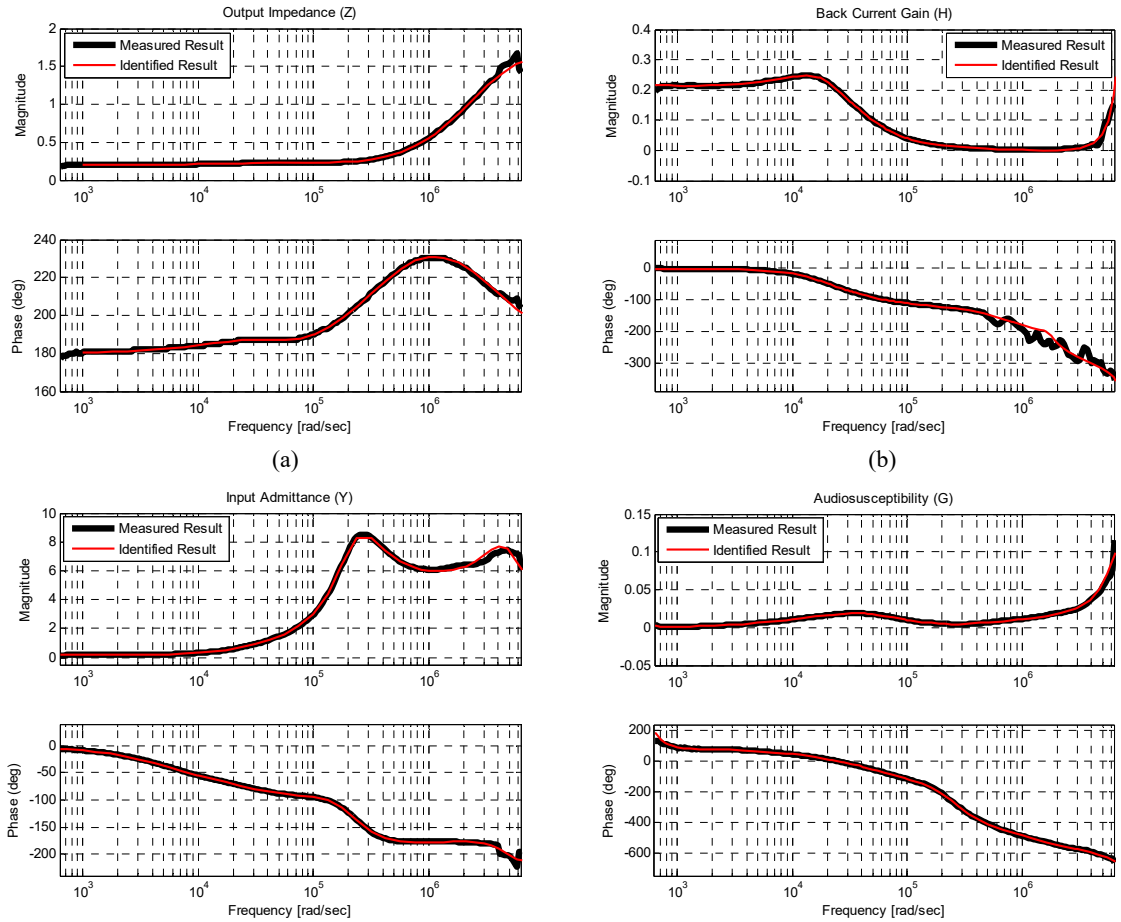

Fig. 7. Frequency response comparison of (a) Output impedance (b) Back current gain (c) Input admittance (d) Audiosusceptibility.

$$\begin{bmatrix} x'(t) \\ y(t) \end{bmatrix} = \begin{bmatrix} A & B \\ C & D \end{bmatrix} \begin{bmatrix} x(t) \\ u(t) \end{bmatrix} \tag{4}$$

For a given stable state-space system, the Hankel singular values are calculated as the square root of the product of controllability and observability gramians [19].

$$\sigma_i = \sqrt{\lambda_i(W_c W_o)} \tag{5}$$

In equation (5), the Hankel singular values of the system are represented by $\sigma_{\mathrm{i}} = \{\sigma_1, \sigma_2, \sigma_3, \ldots\ldots \sigma_{\mathrm{n}}\}$, the eigenvalues are represented by $\lambda_{\mathrm{i}} = \{\lambda_1, \lambda_2, \lambda_3, \ldots\ldots \lambda_{\mathrm{n}}\}$, while W_c and W_o represent the controllability and observability gramians, which can be obtained by solving the following Lyapunov equation:

$$\begin{aligned} AW_c + W_c A^T &= -BB^T \\ AW_c + W_c A^T &= -BB^T \end{aligned} \tag{6}$$

The Hankel singular values are represented as the entries of a diagonal matrix in descending order

$$\sigma_{\mathrm{i}} = diag(\sigma_1, \sigma_2, \cdots\cdots, \sigma_{\mathrm{m}}, \sigma_{\mathrm{m+1}}, \cdots\cdots, \sigma_{\mathrm{n}}) \tag{7}$$

where $\sigma_1 > \cdots \sigma_{\mathrm{m}} > \sigma_{\mathrm{m+1}} > \cdots \sigma_{\mathrm{n}} > 0$

For system order reduction, if the values in (7) are related so that $\sigma_{\mathrm{m+1}} \ll \sigma_{\mathrm{m}}$, this implies that the states related to $\sigma_{\mathrm{m+1}}, \ldots, \sigma_{\mathrm{n}}$ are less controllable and less observable than the preceding states, i.e. $\sigma_1 \ldots \sigma_{\mathrm{m}}$. This means that the states up to σ_{m} are the dominant states of the system, while the remainder of the states have a negligible effect upon the overall dynamic response of the system. Thus, these states can be discarded without a loss of the main characteristics of a system.

In order to have a uniform criterion for keeping the maximum energy states while neglecting the others it is decided to retain the states that add up to have 80% or more of the total energy of the system. If α_{x} represents the percentage contribution of state σ_{x}, then it can be written as:

$$\alpha_1 + \alpha_2 +, \cdots\cdots, \alpha_{\mathrm{m}} \geq 80\% \tag{8}$$

By having a plot of the energy contained by each state, it is possible to have an idea of the maximum energy states of the system. For transfer functions with unstable poles, only the Hankel singular values of the stable part are computed, and the entries of the corresponding unstable modes are set to infinity.

MATLAB is used to get a plot for the energy of each state. The label *stable modes*, indicates that all of the poles of the transfer function are stable. The following MATLAB command gives numeric values of the energy associated with each state.

state_energy = hsvd (TF_{fo})

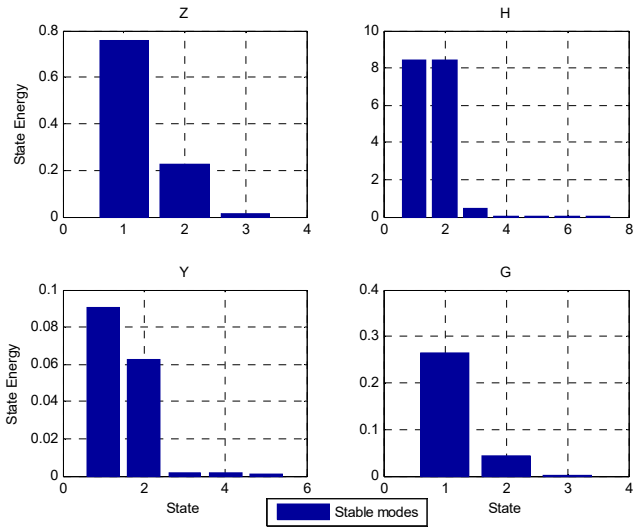

Fig. 8. Hankel singular values graph for buck converter.

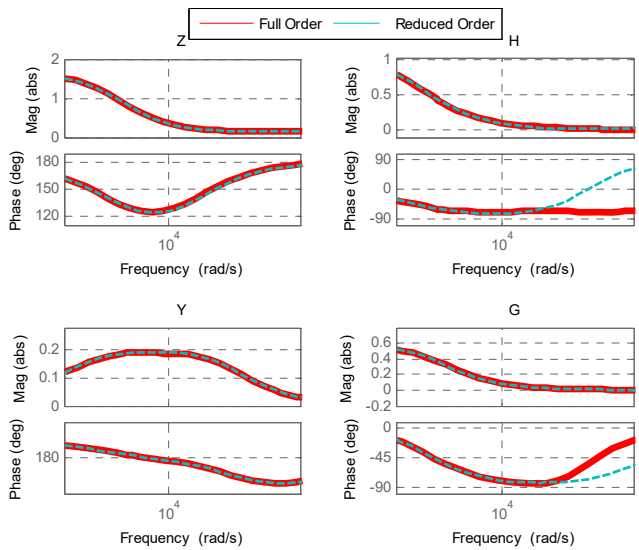

Fig. 9. Full and reduced order plots for buck converter.

The full and reduced order models obtained through system identification are compared and presented in Fig. 9.

Using the *state_energy* vector, the percentage contribution of each state is computed and the states that add up to 80% energy or more are retained, while the remaining states are discarded. The states selection criterion developed for order reduction is applied to three different type of converters. It will be shown next that it works equally well for each type, which suggests the effectiveness of the proposed method.

The model order reduction criterion is applied to the Hankel singular values graph shown in Fig. 8 for a buck converter. In each case, only the first two states are sufficient to meet the chosen limit. Therefore, the reduced order identified transfer functions are of second order.

A Hankel singular values graph for a boost converter is shown in Fig. 10. Here only the first two or three states fulfill the required state energy limit. Therefore, the reduced order identified transfer functions are of second or third order.

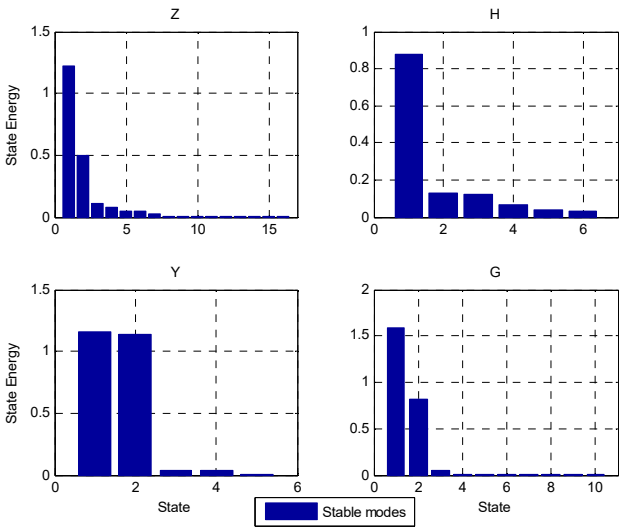

Fig. 10. Hankel singular values graph for boost converter.

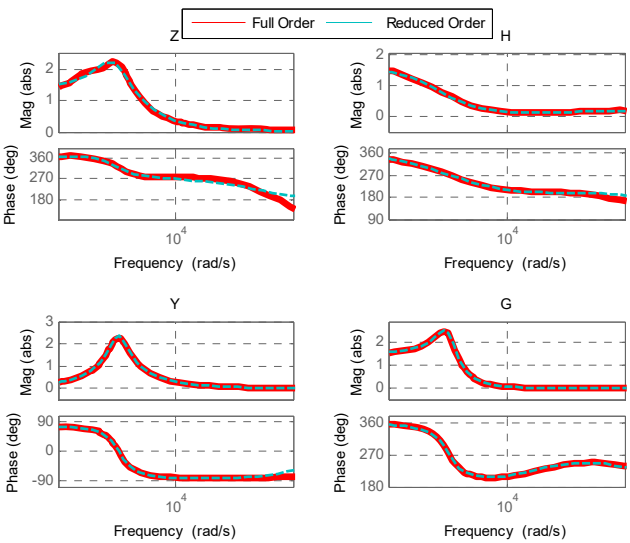

Fig. 11. Full and reduced order plots for boost converter.

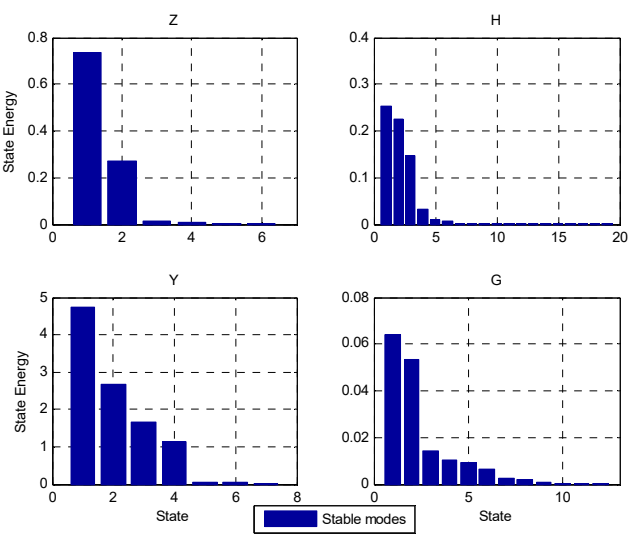

Fig. 12. Hankel singular values graph for Vicor converter.

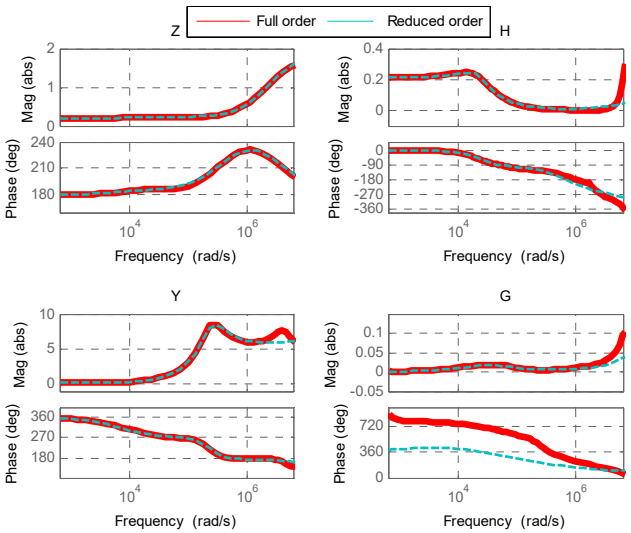

Fig. 13. Full and reduced order models for Vicor converter.

TABLE III
COMPARISON OF FULL AND REDUCED ORDER TRANSFER FUNCTIONS

	Buck		Boost		Vicor	
Transfer Function	Full	Reduced	Full	Reduced	Full	Reduced
Z_o	3	2	16	2	6	2
H_i	7	2	6	3	19	3
Y_i	5	2	5	2	7	3
G_o	3	2	10	2	12	3

The full and reduced order models obtained through system identification are compared and presented in Fig. 11.

A Hankel singular values graph for a *V24C5C100BL* converter is shown in Fig. 12. Here the first two or three states fulfill the required state energy limit. Therefore, the reduced order identified transfer functions are of second or third order.

The full and reduced order models obtained through system identification are compared and presented in Fig. 13.

The full and reduced order models shown above match very well except for a slight mismatch in few of the phase plots. It can be further improved by increasing the set limit for the percentage contribution of the states. However, the cost will be in terms of increase in the number of states in the reduced order models.

A comparison of the full and reduced order identified transfer functions for the three converters is given in Table III.

It is quite evident that even after the system order reduction, the reduced order transfer functions match very well with the full order transfer functions.

A comparison of the simulation speed for the full vs. reduced order transfer functions based behavioral models constructed in MATLAB/SIMULINK is given in Table IV. When computing the simulation time, the parameters e.g. step size and solver type, effect the speed. Therefore, these computations are made by having all the parameters same for each model.

TABLE IV
COMPARISON OF SIMULATION SPEED

Converter	Full	Reduced	Percentage decrease
Buck	0.203s	0.145s	28.6%
Boost	0.633s	0.117s	81.5%
Vicor	0.261s	0.104s	60.2%

Table IV confirms a significant decrease in the simulation time for the reduced order transfer functions based models. These can be highly effective in large distributed power systems, resulting in short simulation time.

VII. DYNAMIC ANALYSIS

Both the full and reduced order transfer functions obtained via system identification need to be validated to determine the effectiveness of the model order reduction. A two port network based behavioral model of the system is build using the procedure described in [20]. For the validation and comparison of the full and reduced order models, a step load current test is applied to both models and the results obtained are compared for the three converters as shown in Fig. 14 (a, b and c). The time domain results clearly show very good agreement between the full order and the reduced order system responses, which validates the effectiveness of the order reduction for the measured transfer functions.

VIII. STABILITY ANALYSIS

An analysis of the distributed power system's stability can be done by making use of small signal impedance based models [21], [22]. This is based upon analyses of the equivalent source output impedance and load input admittance. The criterion is valid for the small-signal stability analysis of a distributed power system with multiple interconnected systems. According to this criterion, if Z_s and Y_L represent the source output impedance and load input admittance at the interface, as shown in Fig. 14, the corresponding small signal transfer function is represented as given in equation (9).

$$\frac{V_o(s)}{V_i(s)} = \frac{Z_L(s)}{Z_L(s)+Z_s(s)} = \frac{1}{1+\frac{Z_s(s)}{Z_L(s)}} \tag{9}$$

The system is stable if the impedance ratio $Z_s(s)/Z_L(s)$ satisfies the Nyquist criterion.

This shows that the stability of the system depends upon the ratio called the minor loop gain $L(s)$ as shown in equation (10) [23].

$$L(s) = \frac{Z_s(s)}{Z_L(s)} = Z_s(s)\, Y_L(s) \tag{10}$$

Therefore, the Nyquist stability criterion can be applied to

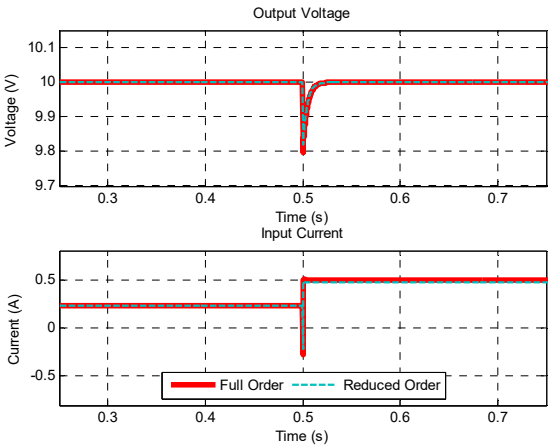

(a)

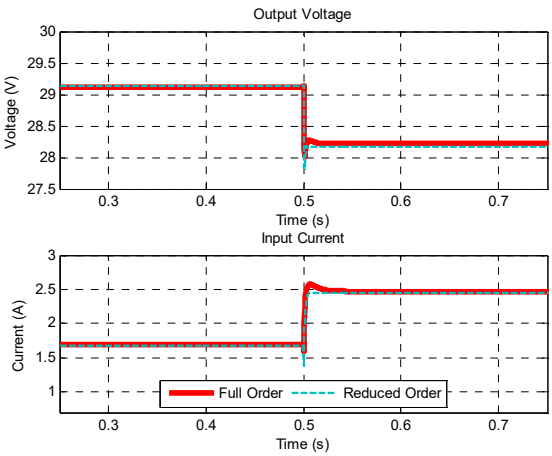

(b)

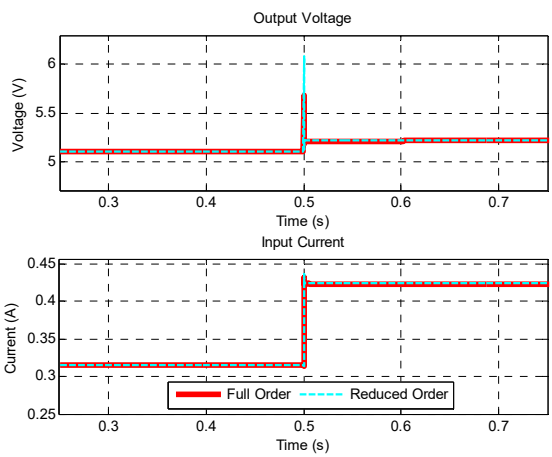

(c)

Fig. 14. Behavioral model response for full and reduced order transfer functions (a) Buck converter (b) Boost converter (c) Vicor converter.

$L(s)$ for the stability analysis of interconnected power modules.

Fig. 15 shows a general view of two interconnected subsystems.

For three converters, the Nyquist diagram of the return ratio is shown in Fig. 16 (a, b and c).

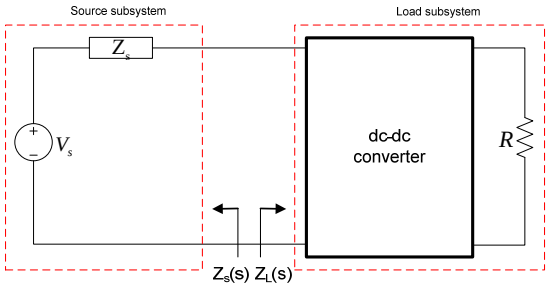

Fig. 15. Source and load subsystems interaction.

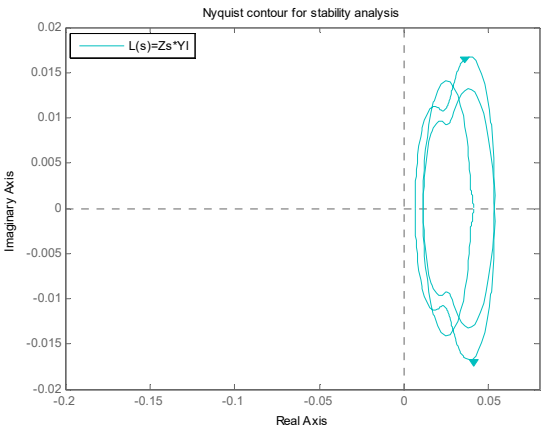

(a)

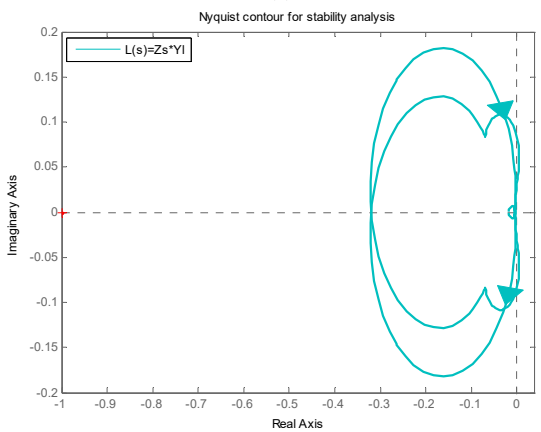

(b)

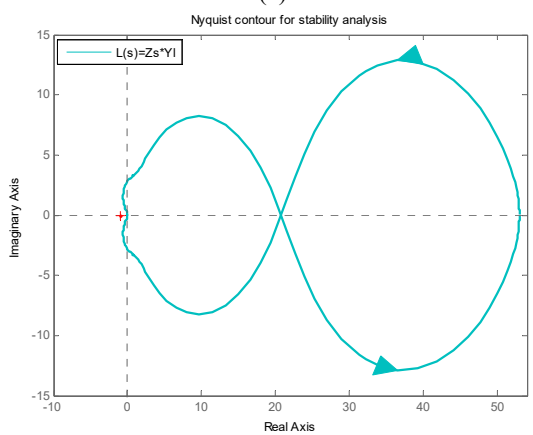

(c)

Fig. 16. Stability analysis using Nyquist diagram (a) Buck converter (b) Boost converter (c) Vicor converter.

For each of the three converters, the interaction between the source and load sub system is stable as shown by the non-encirclement of point (-1, 0) in the return ratio Nyquist diagram.

IX. CONCLUSIONS

The model order reduction technique presented in this paper finds application in DPSs involving numerous converters, most of which are from different vendors with very limited information available on the internal design and parameters. These converter are integrated to make large DPSs. Due to the lack of information concerning the internal structure of these black-box type converters it is not possible to construct analytical models. Therefore, a behavioral modeling procedure is adopted for their analysis. The behavioral modeling based system level analysis is very suitable for DPSs. Since the originally identified models are of high order, to increase the computational efficiency and to reduce the simulation time, the model order reduction technique can be effectively employed. This work shows that high order behavioral models can be systematically reduced to lower dimensions, which helps speed up the design process by lowering model setup and simulation time. The purpose of using three different converters is to validate the effectiveness of the presented model order reduction technique and the procedure to select the high energy states for the reduced order models. Along with buck and boost prototypes, a commercial converter which serves as a complete black-box is used for the validation of the presented model order reduction technique. The close agreement of the results for the full vs. reduced order behavioral models verifies the effectiveness of the model order reduction technique. The measured frequency responses for all three converter systems are used to analyse the dynamic interaction between the source and the load using Bode plots and Nyquist diagrams. In each case the Nyquist contour does not encircle the (-1, 0) point, which indicates the stable operation of the converters.

REFERENCES

[1] L. Man and C. Farcas, "Switch mode power supply used for medical applications – packaging and thermal analysis," in *IEEE 16th International symposium for design and technology in electronic packaging (SIITME)*, pp. 275-278, 2010.

[2] P. D. Nonn, A. H. Seltzman, and J. K. Andrson, "Design of an 80kV, 40A resonant switch mode power supply for pulsed power applications," in *IEEE International Power modulator and high voltage conference (IPMHVC)*, pp. 84-87, 2012.

[3] C. E. C Ortiz, "Circuit oriented average modeling of switching power converters," in *European Conference on Power Electronics and Applications*, pp.1-10, 2005.

[4] J. Sun, "Characterization and performance comparison of ripple-based control for voltage regulator modules," *IEEE Trans. Power Electron.*, Vol. 21, No. 2, pp. 346-353, Mar. 2006.

[5] L. Arnedo, R. Burgos, F. Wang, and D. Boroyevich, "Black-box terminal characterization modeling of DC-to-DC converters," in *Proc. of Twenty Second Annual IEEE Applied Power Electronics Conference and Exposition (APEC 07)*, pp. 457-463, 2007.

[6] D. Boroyevich, R. Burgos, L. Arnedo, and F. Wang, "Synthesis and integration of future electronic power distribution systems," in *Proc. of Power Conversion Conference (PCC)*, pp. 1-8, 2007.

[7] D. Izquierdo, R. Azcona, F. J. Lopez del Cerro, C. Fernandez, and B. Delicado, "Electrical power distribution system (HV270DC), for application in more electric aircraft," in *Proc. of twenty-fifth Annual IEEE Applied Power Electronics Conference and Exposition (APEC)*, pp. 1300-1305, 2010.

[8] A. Emadi, Y. J. Lee, and K. Rajashekara, "Power electronics and motor drives in electric, hybrid electric, and plug-in hybrid electric vehicles," *IEEE Trans. Ind. Electron.*, Vol. 55, No. 6, pp. 2237-2245, Jun. 2008.

[9] X. Zheng, H. Ali, X. Wu, O. Kuseso, S. Khan, and H. Zaman, "Frequency response measurements based reduced order identification for dc-dc converter," in *Proc. of International Conference on Intelligent Systems Engineering (ICISE)*, pp. 78-82, 2016.

[10] P.G. Maranesi, V. Tavazzi, and V. Varoli, "Two-port characterization of PWM voltage regulators at low frequencies," *IEEE Trans. Ind. Electron.*, Vol. 35, No. 3, pp. 444-450, Aug. 1988.

[11] T. Suntio and I. Gadoura, "Use of unterminated two-port modeling technique in analysis of input filter interactions in telecom DPS Systems," in *Proc. 24th IEEE International Telecommunications Energy Conference* (INTELEC), pp. 560–565, 2002.

[12] T. Suntio, "Unified average and small-signal modeling of direct-on-time control," *IEEE Trans. Ind. Electron.*, Vol. 53, No. 1, pp. 287-295, Feb. 2006.

[13] Agilent Technologies, *Keysight - Electronic Measurement Products, E5061B*. http://www.agilent.com, 2016.

[14] G. C. Verghese and V. J. Thottuvelil, "Aliasing effects in PWM power converters," in *30th Annual IEEE Power Electronics Specialists Conference (PESC 99),* Vol. 2, pp. 1043-1049, 1999.

[15] L. Ljung, *System Identification: Theory for the User*, 2nd ed., Prentice Hall, 1999.

[16] Ridley Engineering, *Frequency Response Measurements*, Design Center Library, Switching Power Magazine, http://www.ridleyengineering.com, 2016.

[17] Vicor, *V24C5C100BL Datasheet*, http://cdn.vicorpower.com/documents/datasheets/ds_24vin-micro-family.pdf, 2016.

[18] J. D. Owens and P. L. Chapman, "Automatic generation of accurate low-order models for magnetic devices," *IEEE Trans. Power Electron.*, Vol. 20, No. 4, pp. 732–742, Jul. 2005.

[19] C. Kenney and G. Hewer, "Necessary and sufficient conditions for balancing unstable systems," *IEEE Trans. Autom. Control,* Vol. AC-32, No. 2, pp. 157-160, Feb. 1987.

[20] I. Cvetkovic, D. Boroyevich, P. Mattavelli, F. C. Lee, and D. Dong, "Unterminated small-signal behavioral model of DC-DC converters," *IEEE Trans. Power Electron.*, Vol.

28, No. 4, pp. 1870-1879, Apr. 2013.
[21] C. M. Wildrick, F. C. Lee, B. H. Cho, and B. Choi "A method of defining the load impedance specification for a stable distributed power system," *IEEE Trans. Power Electron.*, Vol. 10, No. 3, pp. 280-285, May 1995.
[22] J. Sun, "Small-signal methods for AC distributed power systems- a review," *IEEE Trans. Power Electron.*, Vol. 24, No. 11, pp. 2545-2554, Nov. 2009.
[23] R. D. Middlebrook, "Input Filter Considerations in Design and Application of Switching Regulators," in *Proc. IEEE Industrial Applications Society Annual Meeting*, pp. 366-382, 1976.

Husan Ali received his B.Sc. degree in Electrical Engineering and his M.Sc. degree in Communication and Electronics Engineering from the University of Engineering and Technology (UET), Peshawar, Pakistan, in 2009 and 2012, respectively. He received his M.Sc. degree in Electrical Engineering from Northwestern Polytechnical University (NPU), Xi'an, China, in 2014, where he is presently working towards his Ph.D. degree in the School of Automation. His current research interests include behavioral modeling and analysis of distributed power systems.

Xiancheng Zheng received his B.Sc., M.Sc. and Ph.D. degrees in Electrical Engineering from Northwestern Polytechnical University (NPU), Xi'an, China, in 1998, 2001 and 2011, respectively. In 2001, he joined NPU, where he is presently working as an Associate Professor in the School of Automation. His current research interests include bidirectional AC-DC converter designs for aircraft electrical power systems, and silicon carbide based high power density DC-DC and DC-AC converters.

Xiaohua Wu received her B.Sc., M.Sc. and Ph.D. degrees in Electrical Engineering from Northwestern Polytechnical University (NPU), Xi'an, China, in 1991, 1994 and 2004, respectively. In 1994, she joined NPU, where she is presently working as a Professor in the School of Automation. Her current research interests include modern control in power electronics, the modeling and simulation of power electronic devices and the application of power electronics.

Haider Zaman received his B.Sc. degree in Electronics Engineering from the University of Engineering and Technology (UET), Abbottabad, Pakistan, in 2008; and his M.Sc. degree in Electrical Engineering from the COMSATS Institute of Information Technology (CIIT), Abbottabad, Pakistan, in 2013. He is presently working towards his Ph.D. degree in the School of Automation, Northwestern Polytechnical University, Xi'an, China. His current research interests include silicon carbide based high power density DC-DC and DC-AC converters.

Shahbaz Khan received his B.Sc. degree in Electronics Engineering from the University of Engineering and Technology (UET), Abbottabad, Pakistan, in 2010; and his M.Sc. degree in Electrical Engineering from Northwestern Polytechnical University (NPU), Xi'an, China, in 2014, where he is presently working towards his Ph.D. degree in the School of Automation. His current research interests include the modeling of AC-DC-AC converters and their stability analysis.